JOURNAL OF THERMOPHYSICS AND HEAT TRANSFER
Vol. 21, No. 1, January–March 2007

Application of the Hot-Plane Method to Low-Density Thermal Insulators

R. Coquard*
Centre Scientifique et Technique du Bâtiment, 38400 Saint Martin d'Hères, France
and
D. Baillis†
Centre Thermique de Lyon, 69621 Villeurbanne Cedex, France

DOI: 10.2514/1.21610

The use of the hot-plane method for thermal conductivity measurement has recently shown a significant increase. However, this method is theoretically inapplicable to materials for which radiative heat transfer is important, such as low-density thermal insulators. To better understand the influence of the radiative contribution, we developed a three-dimensional simulation of transient coupled heat transfer and made hot-plane measurements on low-density expanded polystyrene foam. The analysis of theoretical and experimental results shows that classical hot-plane apparatuses are poorly adapted to low-density insulators. However, if a hot-plane apparatus with sufficiently large dimensions and low thermal inertia is used, the estimated equivalent thermal conductivity is in close agreement with that estimated by the guarded hot-plate method.

Nomenclature

$\boldsymbol{a}_x$, $\boldsymbol{a}_y$, $\boldsymbol{a}_z$	=	unit vectors along the x, y, and z coordinates
b_1, b_2, b_3	=	constants for the theoretical effective conductivity of foams
C	=	specific heat of the surrounding material, J/kg/K
E	=	thermal effusivity of the porous material, J/m^2/K/s$^{1/2}$
h	=	thickness of the hot plane, μm
$I(x, y, z, \theta, \varphi)$	=	radiant intensity at point x, y, or z in the direction (θ, φ), W/m^2/sr
$I^0(T)$	=	radiant intensity emitted by a black body at T, W/m^2/sr
$i_{\lim 1}$, $i_{\lim 2}$ and $j_{\lim 1}$, $j_{\lim 2}$	=	number of the nodes delimiting the plane
k	=	thermal conductivity, W/m/K
L	=	length of the square plane, m
n_d	=	number of directions of the angular discretization
nX, nY, nZ	=	number of spatial discretization points along the x, y, and z coordinates
$P(\nu)$	=	phase function with azimuthal symmetry for the scattering from direction (θ', φ') to direction (θ, φ)
$\boldsymbol{q}$	=	heat flux, W/m^2
Q	=	heating power per unit area, W/m^2
R_c	=	thermal contact resistance, m^{2}K/W
t	=	heating time, s
T	=	temperature, K
T_{init}	=	uniform temperature of the material at $t = 0$ s, K
w^m	=	weighting factor for the mth direction of the angular discretization
W	=	heating power dissipated by the Joule effect in the plane, W
x	=	coordinate along x axis
y	=	coordinate along y axis
z	=	coordinate along z axis
β	=	extinction coefficient of the porous material, m^{-1}
Δx	=	length of discretized nodes along the x axis
Δy	=	length of discretized nodes along the y axis
Δz	=	length of discretized nodes along the z axis
ε_p	=	emissivity of the plane
η	=	direction cosine along the x coordinate
θ	=	azimuthal angle of the radiant intensity, rad
κ	=	absorption coefficient of the porous material, m^{-1}
λ	=	wavelength of radiation, μm
μ	=	direction cosine along the z coordinate
$\nu = \mu\mu' + \eta\eta' + \xi\xi'$	=	cosine of the angle between incident and scattering directions
ξ	=	direction cosine along the y coordinate
ρ	=	density of the foam, kg/m^3
ρ_p	=	density of the material constituting the hot plane, kg/m^3
σ	=	scattering coefficients of the porous material, m^{-1}
σ_{SB}	=	Stefan–Boltzmann constant ($\approx 5.67 \times 10^{-8}$ W/m^2/K^4)
φ	=	polar angle of the radiant intensity, rad
Ω	=	solid angle, sr
Ω_p	=	electrical resistance of the plane, Ω
$\omega = \sigma/\beta$	=	scattering albedo

Subscripts

air	=	of air
c	=	conductive
cst	=	of constantan
eq	=	equivalent
hot	=	estimated in classical hot-plane measuring method
i, j, k	=	at node i, j, or k

Received 7 December 2005; revision received 28 August 2006; accepted for publication 2 September 2006.

*24 rue Joseph Fourier; remi.coquard1@insa-lyon.fr.
†UMR CNRS 5008, Domaine Scientifique de la Doua, INSA de Lyon, Bâtiment Sadi Carnot, 9 rue de la Physique; dominique.baillis@insa-lyon.fr.

kpt	=	of kapton
m	=	measured
max	=	maximal coordinate
p	=	of the plane
PS	=	of polystyrene
r	=	radiative
ROSS	=	from Rosseland approximation
th	=	theoretical
1 or 2	=	at time t_1 or t_2

Superscripts

ana	=	analytical results
l	=	iteration level during the discrete ordinates method
m	=	relative to the *m*th direction of the angular discretization
num	=	numerical results
t	=	at time *t*
x	=	along the x coordinate
y	=	along the y coordinate
z	=	along the z coordinate
′	=	relative to the scattering direction

I. Introduction

THE accuracy of thermal properties measurement takes on particular importance in numerous physical, chemical, or medical applications, given that it has a direct influence on the estimation of heat losses or temperature rise. For purely conductive materials, two parameters entirely describe the thermal behavior: the thermal conductivity and the specific heat. For the estimation of the thermal conductivity, the principle of the guarded hot-plate method [1] is to measure the heat flux passing through a slab of material subjected to a one-dimensional steady-state heat transfer. This technique gives very accurate results. Nevertheless, it is restrictive, given that the slab must have large and standard dimensions and that it requires especially long measurement durations.

During the last two decades, there has been significant development of transient methods for measurement of thermophysical properties over a broad range of materials. We can cite, for example, the flash method [2,3], which has recently shown strong development. In particular, Lazard et al. [4] studied the application of this method to measure the intrinsic diffusivity of semitransparent media in which radiative heat transfer is significant. New techniques, such as the hot-disk method described in detail in [5], are also being developed. However, the transient method of measuring the thermal conductivity, which has been the most widely used for a broad range of materials, is the widely known hot-wire method or hot-line-source technique. Numerous studies [6,7] have used this technique, because it is practical and the numerical treatment of the measured data is very simple. The hot-plane method is another transient technique similar to the hot-wire method. It has been used in [8,9]. However, it is, at present, not well known, although it has the same advantages as the hot-line-source technique. Indeed, it is relatively simple and fast, as it is based on the transient measurement of the temperature rise of a uniformly heated plane. Moreover, the measurement can be made on samples with any shape and relatively small size. However, the hot-plane method, which is based on Fourier's diffusion law, is restricted to opaque materials; it is not theoretically applicable to materials for which radiative heat transfer occurs, such as low-density thermal insulators. It would be very interesting if this method could be extended to such media that constitute a great part of the thermal insulators used in the building industry, (e.g., expanded polystyrene (EPS) foams and light fibrous materials).

To evaluate the influence of radiative heat transfer on hot-plane measurement, we have conducted a theoretical and experimental study on low-density EPS foam for which usual measurements lead to noticeable differences from the standard guarded hot-plate method. The aim is to propose, if possible, an extension of the classical hot-plane technique to this type of porous material. At first, we review the principles of the method and the governing equations for an infinite plane with negligible inertia in a purely conductive medium. Then, we describe the theoretical model developed to take into account the influence of coupling between conduction and radiation, the inertia of the plane, the thermal contact resistance between the plane and the medium, and the edge effects on the temperature rise. The 3-D energy equation and the radiative transfer equation are solved numerically. The properties of the EPS foam, used for the calculation, were determined theoretically in a previous study [10] that was interested in modeling steady-state heat transfer in this thermal insulator. The radiative properties were calculated from measured structural characteristics, such as density or mean cell diameter, using the independent scattering hypothesis. The validity of the model used has been checked by comparing experimental transmittance and reflectance measurements for thin slabs of foam, with the calculated values obtained using the theoretical monochromatic radiative properties. Conductive properties k_c have also been determined from a validated theoretical model from the literature, taking into account the conductivity of the constituents and the morphology of the foam. The analysis of the theoretical results permits us to explain the noticeable differences between the thermal conductivity measured by the classical hot-plane method and that measured by the guarded hot-plate method.

II. Governing Equations

A. Infinite Plane in a Purely Conductive Medium

The principle of the standard transient hot-plane method is to heat a large, thin plate immersed in a sample of the material studied and measure the plate's temperature rise. The heating of the plate generates a 1-D transient temperature field in the material. This transient temperature field is closely related to the diffusivity of the material. Indeed, the heat balance is governed by the energy equation. In the case of heat transfer in Cartesian coordinates in a purely conductive medium, the equation is expressed in the form

$$\rho C \frac{\partial T}{\partial t} = -\nabla \boldsymbol{q}_c = \frac{\partial}{\partial z}\left(k_c \frac{\partial T}{\partial z}\right) \tag{1}$$

Assuming that 1) the medium is at a uniform temperature before the beginning of heating, 2) there is no thermal resistance at the contact area between the plane and the medium, and 3) the hot plane is infinite and has a negligible inertia, the boundary conditions are

$$\forall\ z \quad \text{when } t \le 0, \qquad T(z,t) = T_{\text{init}} \tag{2a}$$

$$\text{for } z = h/2 \quad \text{and} \quad \forall\ t, \qquad -k_c\left(\frac{\partial T}{\partial z}\right)_{z=h/2} = \dot{Q} \tag{2b}$$

$$\text{for } z \to \infty \quad \text{and} \quad \forall\ t, \qquad \lim_{z\to\infty} T(z,t) = T_{\text{init}} \tag{2c}$$

Assuming that the properties of the medium are independent of the temperature, when t is sufficiently large, the solution of the energy equation for the temperature rise of the hot plane is given by numerous authors, such as Carslaw and Jaeger [11]:

$$T_p(t) - T_{\text{init}} = \frac{2\dot{Q}}{\sqrt{\pi k_c \rho C}}\sqrt{t} = \frac{2\dot{Q}}{\sqrt{\pi}E}\sqrt{t} \tag{3}$$

Equation (3) shows that it is sufficient to know the temperatures T_1 and T_2 of the plane at different times t_1 and t_2 to determine the thermal effusivity and then the thermal conductivity of the material. This results in

$$k_c = \frac{E^2}{\rho C} = \left(\frac{2\dot{Q}(\sqrt{t_1} - \sqrt{t_2})}{\sqrt{\pi}(T_1 - T_2)\sqrt{\rho C}}\right)^2 \tag{4}$$

B. Finite Plane with Thermal Inertia in a Semitransparent Medium

In practice, the inertia of the plane is not negligible, the contact between the plane and the surrounding medium is not perfect, and the plane's area A is limited. Thus, to model the edge effects, the temperature distribution in the medium, as well as the temperature of the plate, must be a function of the x, y, z coordinates and t (see Fig. 1).

1. Energy Equation

The heat balance in a semitransparent, conductive (but nonconvective) medium is still governed by the energy equation, which has to take into account the radiative heat transfer:

$$\rho C(\partial T/\partial t) = -\nabla(\boldsymbol{q}_t) = -[\nabla(\boldsymbol{q}_r) + \nabla(\boldsymbol{q}_c)] \tag{5}$$

Moreover, in the case of three-dimensional heat transfer in Cartesian coordinates in a homogeneous and isotropic medium, the conductive flux is expressed in the form

$$\boldsymbol{q}_c = -k_c\left(\frac{\partial T}{\partial x}\boldsymbol{a}_x + \frac{\partial T}{\partial y}\boldsymbol{a}_y + \frac{\partial T}{\partial z}\boldsymbol{a}_z\right) \tag{6}$$

Then, if we assume that the variations $\partial k_c/\partial x$, $\partial k_c/\partial y$, and $\partial k_c/\partial z$ are negligible, we have

$$\nabla(\boldsymbol{q}_c) = -k_c\left(\frac{\partial^2 T}{\partial x^2} + \frac{\partial^2 T}{\partial y^2} + \frac{\partial^2 T}{\partial z^2}\right) \tag{7}$$

2. Radiative Transfer Equation

Regarding radiative heat transfer, the radiative heat flux is related to the intensity field $I(x, y, z, \theta, \varphi)$ in the porous medium:

$$\begin{aligned} &\boldsymbol{q}_r = q_r^x\boldsymbol{a}_x + q_r^y\boldsymbol{a}_y + q_r^z\boldsymbol{a}_z \quad \text{with} \\ &q_r^z(x, y, z) = \int_{\Omega=4\pi} I(x, y, z, \theta, \varphi)\mu \, \mathrm{d}\Omega; \\ &q_r^x(x, y, z) = \int_{\Omega=4\pi} I(x, y, z, \theta, \varphi)\eta \, \mathrm{d}\Omega \end{aligned} \tag{8}$$

$$\begin{aligned} &q_r^y(x, y, z) = \int_{\Omega=4\pi} I(x, y, z, \theta, \varphi)\xi \, \mathrm{d}\Omega \quad \text{and} \\ &\nabla(\boldsymbol{q}_r) = \frac{\partial q_r^x}{\partial x} + \frac{\partial q_r^y}{\partial y} + \frac{\partial q_r^z}{\partial z} \end{aligned} \tag{9}$$

where $\boldsymbol{a} = x\boldsymbol{a}_x + y\boldsymbol{a}_y + z\boldsymbol{a}_z$. The direction cosines along the x, y, and z axes are $\eta = \sin\theta\cos\varphi$, $\xi = \sin\theta\sin\varphi$, and $\mu = \cos\theta$, respectively (see Fig. 1).

The radiation intensity field is governed by the radiative transfer equation (RTE), which takes into account emission and absorption and scattering of radiation by the participating medium. For 3-D radiative transfer in an isotropic material with azimuthal symmetry, this equation is

$$\begin{aligned} &\mu\frac{\partial I(x, y, z, \theta, \varphi)}{\partial z} + \eta\frac{\partial I(x, y, z, \theta, \varphi)}{\partial x} + \xi\frac{\partial I(x, y, z, \theta, \varphi)}{\partial y} \\ &\quad + \beta I(x, y, z, \theta, \varphi) = \kappa I^0(T) + \frac{\sigma}{4\pi}\int_{\Omega'=4\pi} P(\nu)I(x, y, z, \theta, \varphi) \, \mathrm{d}\Omega' \end{aligned} \tag{10}$$

Note that it is necessary to know the temperature field in the medium in order to solve the RTE and to determine the radiative intensity field.

3. Radiative Boundary Conditions

At the interface between the plane and the surrounding medium ($z = h/2$), the boundary conditions of the RTE for an emitting and diffusely reflecting plane for $\mu > 0$, $-L/2 < x < L/2$ and $-L/2 < y < L/2$ are

$$\begin{aligned} I(x, y, h/2, \theta, \varphi) &= \varepsilon_p I^0(T_p) \\ &\quad + \frac{1 - \varepsilon_p}{\pi}\int_{\Omega=2\pi;\mu'<0} I(x, y, h/2, \theta', \varphi')|\mu'| \, \mathrm{d}\Omega' \end{aligned} \tag{11}$$

At the edges of the plane ($x = \pm L/2$ and $-L/2 < y < L/2$ or $y = \pm L/2$ and $-L/2 < x < L/2$), there are similar boundary conditions:

$$\begin{aligned} &I(\pm L/2, y, z, \theta, \varphi) = \varepsilon_p I^0(T_p) \\ &\quad + \frac{1 - \varepsilon_p}{\pi}\int_{\Omega=2\pi} I(\pm L/2, y, z, \theta', \varphi')|\eta'| \, \mathrm{d}\Omega' \\ &\quad \text{for } 0 < z < h/2 \\ &I(x, \pm L/2, z, \theta, \varphi) = \varepsilon_p I^0(T_p) \\ &\quad + \frac{1 - \varepsilon_p}{\pi}\int_{\Omega=2\pi} I(x, \pm L/2, z, \theta', \varphi')|\eta'| \, \mathrm{d}\Omega' \\ &\quad \text{for } 0 < z < h/2 \end{aligned} \tag{12}$$

We also have the following relations for the radiative intensities far from the plane:

$$\begin{aligned} &I(x \to \infty, y, z, \theta, \varphi) = I^0(T_{\text{init}}) \quad \text{for } \eta < 0; \\ &I(x \to -\infty, y, z, \theta, \varphi) = I^0(T_{\text{init}}) \quad \text{for } \eta > 0 \\ &I(x, y \to \infty, z, \theta, \varphi) = I^0(T_{\text{init}}) \quad \text{for } \xi < 0; \\ &I(x, y \to -\infty, z, \theta, \varphi) = I^0(T_{\text{init}}) \quad \text{for } \xi > 0 \\ &I(x, y, z \to \infty, \theta, \varphi) = I^0(T_{\text{init}}) \quad \text{for } \mu < 0 \end{aligned} \tag{13}$$

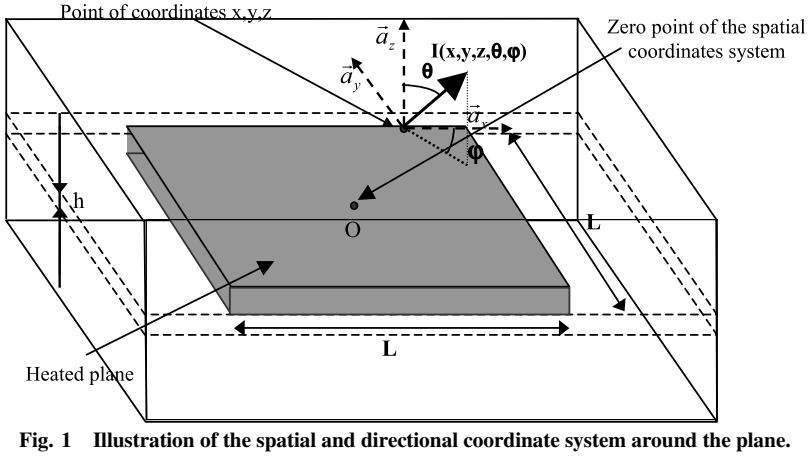

Fig. 1 Illustration of the spatial and directional coordinate system around the plane.

4. Thermal Boundary Conditions

Given that the inertia of the plate and the radiative contribution are not negligible and that the area of the plate is not infinite, the thermal boundary condition around the plane [Eq. (2b)] is also modified to take into account the energy necessary to heat the plane and the radiative flux emitted. We then have

$$\rho_p C_p \Delta x \Delta y \frac{h}{2}\frac{\partial T_p}{\partial t} = \dot{Q}\Delta x\Delta y - q_r^{z=h/2}\Delta x\Delta y + \frac{h}{2}\Delta y k_p\left(\frac{\partial T}{\partial x}\right)_{x=-\Delta x/2} - \frac{h}{2}\Delta y k_p\left(\frac{\partial T}{\partial x}\right)_{x=\Delta x/2} + \frac{h}{2}\Delta x k_p\left(\frac{\partial T}{\partial y}\right)_{y=-\Delta y/2} - \frac{h}{2}\Delta x k_p\left(\frac{\partial T}{\partial y}\right)_{y=\Delta y/2} - \Delta x\Delta y (k_c)_{z=h/2}\left(\frac{\partial T}{\partial z}\right)_{z=h/2} \tag{14}$$

where Δx and Δy are the dimensions of a planar element considered along the x and y coordinates.

Moreover, we have seen that thermal contact between the plane and the surrounding medium is not perfect and, thus, we must introduce a thermal contact resistance at the interface between the plane and the medium. This contact resistance acts on the heat transferred by conduction from the plane to the surrounding medium and modifies the last term on the right-hand side of Eq. (14). In our model, we take into account this thermal resistance by calculating a global thermal resistance that is the sum of the contact resistance and the resistance due to conduction.

The previous boundary conditions, Eqs. (2a) and (2c), remain unchanged, and new boundary conditions far from the plane appear:

$$\lim_{x\to\pm\infty} T(x,y,z,t) = \lim_{y\to\pm\infty} T(x,y,z,t) = \lim_{z\to+\infty} T(x,y,z,t) = T_{\text{init}}; \quad \forall\ t \tag{15}$$

III. Numerical Resolution of the Transient Coupled Heat Transfer

To solve the energy equation (5), and to calculate numerically the variation of the temperature field during the transient heat transfer, we use an implicit time-marching technique. As it is necessary to know the temperature field to solve the RTE and to compute $\nabla \boldsymbol{q}_r$, an internal iterative process should be performed at each time step to produce consistency between the temperature profile and the radiation field. However, when the time interval between two time steps is small ($\Delta t < 0.1$ s in our study), this internal iterative process is superfluous and the temperature field at the new time step could be calculated directly using the radiation intensity field at the previous time step without causing errors. In their study on the temperature rise of a cylindrical piece of glass, Viskanta and Lim [12] use the same simplification.

A. Resolution of the Energy Equation and Computation of the Temperature Field

At each time step, the resolution of the energy equation creates the ability to compute the new temperature distribution in the plate and the surrounding medium from the temperatures and radiation intensity profiles at the previous time step. To solve this equation, a spatial discretization dividing the volume into $nX \times nY \times nZ$ elementary volumes is used (see Fig. 2). To limit the computation time and memory requirement, the heat transfer problem is solved in a finite volume around the plane. Then, the calculations are restricted to $h/2 < z < z_{\max}$, $-x_{\max}/2 < x < x_{\max}/2$, and $-y_{\max}/2 < y < y_{\max}/2$. This volume must be sufficiently important in order for the theoretical temperature of the plane not to be influenced by the value of $z_{\max}$, $x_{\max}$, or $y_{\max}$. At the center of each parallelepipedal elementary volume, there is a node, denoted as i, j, or k. The numerical calculation determines the temperature at each of these nodes. The discretizations along the x and y axes are uniform in the porous medium: $\Delta x = x_{\max}/nX$ and $\Delta y = y_{\max}/nY$. On the other hand, the discretization along the z axis provides narrower volumes near the plane on which important temperature gradients are found:

$$\Delta z_k = \left[\cos\left(\frac{(j-1)\pi}{2nZ}\right) - \cos\left(\frac{j\pi}{2nZ}\right)\right](z_{\max} - h/2) \tag{16}$$

The temperature $T_{i,j,0}$ of the volumes i, j, and 0 for which $i_{\lim 1} < i < i_{\lim 2}$ and $j_{\lim 1} < j < j_{\lim 2}$ correspond to the temperature of the plane denoted as $T_{p,i,j}$. Some additional nodes are placed at the interface between the plane and the surrounding medium and are denoted as $T_{i,j,1/2}$. As the thermal conductivity of the plane is very important compared with the thermal conductivity of the porous medium, we assume that the plane's temperature is uniform and that $T_{i,j,0} = T_{i,j,1/2} = T_{p,i,j}$.

The well-known finite-difference method is used to carry out the numerical resolution of the energy equation in the discretized volume. It is well described in numerous books (e.g., Carlslaw and Jaeger [11]). The method is not detailed here, and the discretization of the energy equation (5) is just illustrated for the nodes containing the porous medium (nodes i, j, $k > 1$):

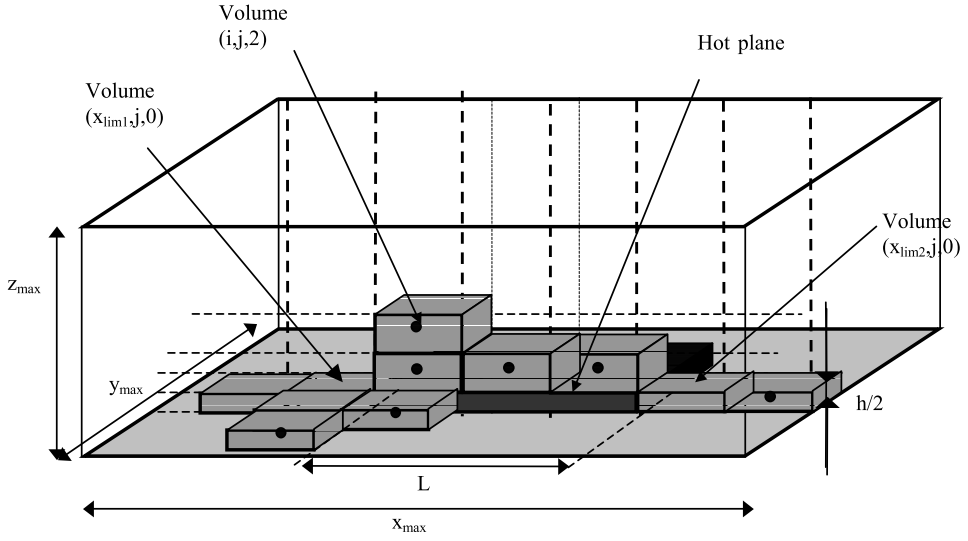

Fig. 2 Illustration of the spatial discretization around the plane.

$$\rho C\frac{T_{i,j,k}^{t+1}-T_{i,j,k}^{t}}{\Delta t}=k_c\frac{T_{i+1,j,k}^{t}-2T_{i,j,k}^{t}+T_{i-1,j,k}^{t}}{\Delta x^2}+k_c\frac{T_{i,j+1,k}^{t}-2T_{i,j,k}^{t}+T_{i,j-1,k}^{t}}{\Delta y^2}+k_c\frac{T_{i,j,k+1}^{t}-2T_{i,j,k}^{t}+T_{i,j,k-1}^{t}}{\Delta z_k^2}-\nabla(\boldsymbol{q}_r)_{i,j,k}^{t} \quad (17)$$

where $\nabla(\boldsymbol{q}_r)_{i,j,k}^{t}$ is the divergence of the radiative heat flux at the nodes i, j, or k at t.

For nodes placed near the hot plane (nodes i, j, or 1, for which $i_{\lim 1} < i < i_{\lim 2}$ and $j_{\lim 1} < j < j_{\lim 2}$), we apply an energy balance that takes into account the thermal contact resistance at the interface between the plane and the surrounding medium.

Finally, the temperature of the plane (nodes i, j, or 0, for which $i_{\lim 1} < i < i_{\lim 2}$ and $j_{\lim 1} < j < j_{\lim 2}$) is computed from the boundary conditions [Eq. (14)] expressed in a discretized form.

B. Resolution of the 3-D RTE Using the Discrete Ordinates Method

To calculate the radiative flux $(\boldsymbol{q}_r)_{i,j}$ and the radiative flux divergence $\nabla(\boldsymbol{q}_r)_{i,j}$ at each point of the spatial discretization, it is necessary to solve the 3-D radiative transfer equation [Eq. (10)] in a porous semitransparent medium. Several numerical methods can be used to solve the RTE. For example, we can cite the spherical harmonics method [13], the zone method of HOTTEL [14], or ray-tracing methods [15]. However, the discrete ordinates method (DOM) is the most frequently used, gives accurate results, and is used in this study. This method was first proposed by Chandrasekar [16] in 1960. The DOM is based on a spatial discretization and on an angular discretization of the space. The angular discretization allows replacing the angular integrals by finite summations over n_d discrete directions m (μ^m, η^m, and ξ^m) with given weighting factors. The spatial discretization must be the same as the one used for the resolution of the energy equation, given that in order to solve the energy equation in a discretized volume, it is necessary to know the divergence of the radiative heat flux at the center of the same volume. The 3-D discrete ordinates solution for a radiatively participating medium in a parallelepipedal enclosure has been widely described, notably by Ayranci and Selçuk [17]. We give the expression of the 3-D RTE [Eq. (10)] according to the angular and spatial discretization:

$$\mu_m\frac{I_{i,j,k+1/2}^{m}-I_{i,j,k-1/2}^{m}}{\Delta z}+\eta_m\frac{I_{i+1/2,j,k}^{m}-I_{i-1/2,j,k}^{m}}{\Delta x}+\xi_m\frac{I_{i,j+1/2,k}^{m}-I_{i,j-1/2,k}^{m}}{\Delta y}=-\beta I_{i,j,k}^{m}+\kappa I^0(T_{i,j,k})+\frac{\sigma}{4\pi}\sum_{m'=1}^{n_d}\mathrm{P}(\nu)\mathrm{I}_{i,j,k}^{m}w_{m'} \quad (18)$$

where $I_{i,j,k}^{m}$ is the radiative intensity at the center of the elementary volumes i, j, and k in the discretized direction m; and $I_{i\pm1/2,j,k}^{m}$, $I_{i,j\pm1/2,k}^{m}$, and $I_{i,j,k\pm1/2}^{m}$ are the radiative intensities at the x, y, and z boundaries of elementary volumes i, j, or k, respectively. Also, $\nu' = \mu^m\mu^{m'} + \xi^m\xi^{m'} + \eta^m\eta^{m'}$.

Similarly, the radiative boundary condition at the interface between the plane and the porous medium [Eq. (11)] could be expressed in discretized form:

$$I_{i,j,1/2}^{m}=\varepsilon_p I^0(T_{p,i,j})+\frac{1-\varepsilon_p}{\pi}\sum_{m';\mu_{m'}<0}I_{i,j,1}^{m'}|\mu^{m'}|w^{m'} \quad \text{for } \mu^m>0 \quad \text{and} \quad j_{\lim 1}<j<j_{\lim 2} \quad (19)$$

This boundary condition, the other boundary conditions [Eq. (13)], and a recursive relation derived from Eq. (18) permit the successive computation of the radiative intensities at all nodes and in all of the discretized directions. The procedure is continued until the convergence criterion

$$\frac{|I_{i,j,k}^{m(l+1)}-I_{i,j,k}^{m(l)}|}{I_{i,j,k}^{m(l)}}<10^{-6}$$

is achieved for all directions and all nodes.

Once the radiation intensity field in the semitransparent medium around the plane has been determined, the radiative flux and its divergence are calculated using the discretized form of Eqs. (8) and (9):

$$(q_r^z)_{i,j,k}=\left[\sum_{m=1}^{n_d}I_{i,j,k}^{m}\mu_m w_m\right];\qquad (q_r^x)_{i,j,k}=\left[\sum_{m=1}^{n_d}I_{i,j,k}^{m}\eta_m w_m\right];\qquad (q_r^y)_{i,j,k}=\left[\sum_{m=1}^{n_d}I_{i,j,k}^{m}\xi_m w_m\right] \quad (20)$$

$$\nabla(\boldsymbol{q}_r)_{i,j,k}=\frac{(q_r^x)_{i+1/2,j,k}-(q_r^x)_{i-1/2,j,k}}{\Delta x}+\frac{(q_r^y)_{i,j+1/2,k}-(q_r^y)_{i,j-1/2,k}}{\Delta y}+\frac{(q_r^z)_{i,j,k+1/2}-(q_r^z)_{i,j,k-1/2}}{\Delta z} \quad (21)$$

C. Validation of the Numerical Method

The numerical resolution of the 3-D radiative problem in Cartesian coordinates has been tested by comparing the results of our model with various published results [17,18] for different media in which only radiative transfer occurs. The accuracy of the numerical method is strongly dependent on the quadrature used for the angular discretization. We have tested different S_N quadratures. The results obtained when using the quadrature points and weights of the S_6 scheme prove to be quite satisfactory,as the difference with the results of the S_8 scheme is always lower than 1% in all cases. Thus, we will use the S_6 quadrature in all the following theoretical calculations.

Concerning the entire 3-D transient radiation/conduction coupling problem, no previous results have been published. Thus, the validity of the numerical solution was checked by carrying out the following computations for two limiting cases: 1) infinite purely conductive medium ($\beta \to \infty$, $k_c = 0.035$ W/m/K) around an infinite plane ($L \to \infty$) with negligible inertia ($\rho_p C_p h \to 0$) and 2) infinite transparent medium ($\beta = 0$, $k_c = 0.035$ W/m/K) around an infinite plane ($L \to \infty$) with negligible inertia ($\rho_p C_p h \to 0$).

The first test case can be solved analytically,as it corresponds to the ideal case described in Sec. III.A. The variation of the temperature of the plane is then given by Eq. (3). To compare the numerical solution with the analytical one, we have carried out two calculations. The first one delivers an exact numerical solution by setting $\boldsymbol{q}_{r_{i,j}}^{t} = \mathbf{0}$ and $(\nabla\boldsymbol{q}_r)_{i,j}^{t} = 0 \ \forall\ i,\ j,\ k$, and t. The second calculation has been carried out by fixing β to a very large value ($\beta = 10^6$ m^{-1}). The other parameters used for the numerical resolution are $\rho_p C_p = 4720$ J/m^3/K, $k_p = 100$ W/m/K, $\rho C =$ 36000 J/m^3/K, $h = 0.0002$ m, $\dot{Q} = 30$ W/m^2, $T_{\text{init}} = 296$ K, $nZ = 60$, and $nX = nY = 20$. Both calculations were carried out by setting $Z_{\max} = 2$ m and $L = 1$ m. We have checked that the values of $Z_{\max}$ and L are sufficiently large in order for the theoretical results to remain independent of their values. For example, the relative difference between the temperature T_p calculated with $Z_{\max} = 10$ m and $L = 5$ m or $Z_{\max} = 2$ m and $L = 1$ m is always lower than 0.01% in the time range of 0–600 s. The results obtained then correspond to those of an infinite medium around an infinite heated plane.

The comparison between analytical and numerical results is shown in Fig. 3. The temperature depicted for the numerical result is the temperature at the center of the plane, and the numerical deviation corresponds to

$$\frac{T_c^{\text{num}}(t)-T_c^{\text{ana}}(t)}{T^{\text{num}}(t)-T_{\text{init}}}$$

where $T^{\text{num}}(t)$ is the temperature predicted by the numerical

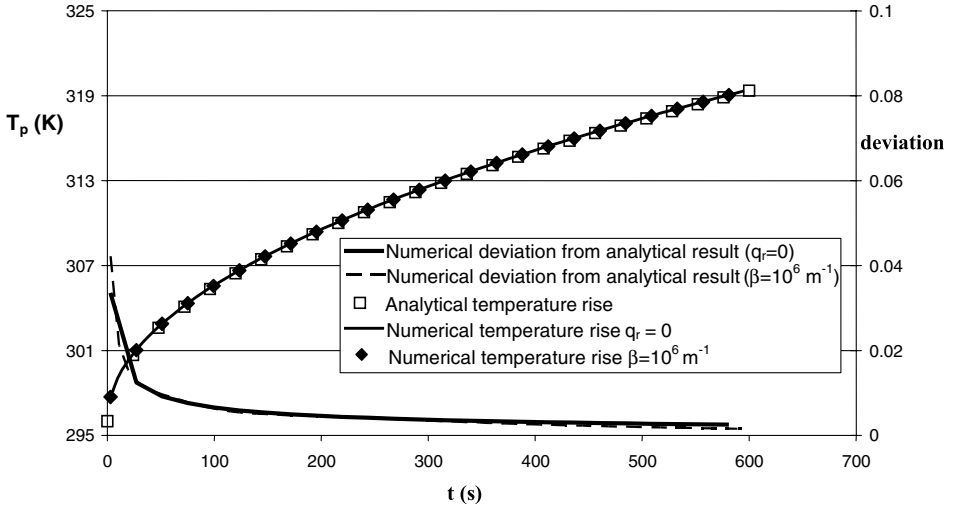

Fig. 3 Evolution of the deviation between analytical and theoretical results for the temperature rise of an infinite plane with no thermal inertia in a purely conductive medium.

simulation with $\boldsymbol{q}^t_{r_{i,j}} = \mathbf{0}$ and $(\nabla \boldsymbol{q}_r)^t_{i,j} = 0$ or $\beta = 10^6$ m^{-1} and $T^{\text{ana}}(t)$ is the temperature given by Eq. (3).

As can be seen, the temperature rise calculated numerically by neglecting radiative heat flux or by setting $\beta = 10^6$ are both very close to the analytical solution, as the relative differences are always lower than 0.5% when $t > 100$ s. We note that the maximum differences between analytical and numerical results are found for very low values of t. This can be explained by the fact that the inertia effects, which are significant at the beginning of the heating, are neglected by the analytical solution, whereas the numerical solutions take into account a low thermal inertia of the plane. Then, the numerical simulation proves to be very accurate when using the spatial discretization and angular quadrature chosen.

The second test case corresponds to the transparency limit $\beta = 0$. Under this assumption, the conductive and radiative contributions can be evaluated separately, as the surrounding medium does not participate in the radiative transfer $[(\nabla \boldsymbol{q}_r)^t_{i,j} = 0]$. There is direct radiative exchange between the plane and the medium at $T = T_{\text{init}}$, and the radiative heat flux emitted by the plane only depends on its emissivity and its local temperature. The flux can be evaluated by the analytical relation:

$$
\begin{aligned}
&(q^z_r)_{i,j,1/2} = \varepsilon_p \sigma_{\text{SB}} (T^{t4}_{p,i,j} - T^4_{\text{init}}) \quad \text{for } j_{\lim 1} < j < j_{\lim 2} \quad \text{and} \\
&\quad i_{\lim 1} < i < i_{\lim 2}; \\
&(q^x_r)_{i\lim 1+1/2,j,0} = \varepsilon_p \sigma_{\text{SB}} (T^{t4}_{p,i\lim 1+1/2,j} - T^4_{\text{init}}); \\
&(q^x_r)_{i\lim 2-1/2,j,0} = \varepsilon_p \sigma_{\text{SB}} (T^{t4}_{p,i\lim 2-1/2,j} - T^4_{\text{init}}) \\
&\quad \text{for } j_{\lim 1} < j < j_{\lim 2}; \\
&(q^y_r)_{i,j\lim 1+1/2,0} = \varepsilon_p \sigma_{\text{SB}} (T^{t4}_{p,i,j\lim 1+1/2} - T^4_{\text{init}}); \\
&(q^y_r)_{i,j\lim 2-1/2,0} = \varepsilon_p \sigma_{\text{SB}} (T^{t4}_{p,i,j\lim 2-1/2} - T^4_{\text{init}}) \quad \text{for } i_{\lim 1} < i < i_{\lim 2}
\end{aligned}
\tag{22}
$$

The results obtained by setting $(\nabla \boldsymbol{q}_r)^t_{i,j,k} = 0$ and using the previous boundary conditions in the purely conductive problem have been compared with those obtained by setting $\beta = 10^{-6}$ m^{-1} in the numerical solution of the conduction–radiation coupling problem. The deviation between the two numerical methods is always lower than 0.001 in the time range of 10–600 s. Thus, the numerical resolution of the radiative problem proves to give satisfactory results.

As a conclusion, the calculations carried out for the two limiting cases show that, when using the spatial discretization $nZ = 20$ and the S_6 quadrature, our numerical method accurately simulates the temperature rise of the plane.

IV. Results and Discussion

To analyze the application of the hot-plane method to low-density thermal insulators, we made a series of experimental measurements on four low-density EPS foams using different hot-plane measuring systems. The results have been compared with theoretical predictions. We used the experimental and theoretical temperature rise of the plane to analyze the evolution of the thermal conductivity k_{hot} estimated in the classical hot-plane measuring method by Eq. (4) for purely conductive media.

$$
k_{\text{hot}} = \left(\frac{2\dot{Q}(\sqrt{t_1} - \sqrt{t_2})}{\sqrt{\pi}(T_1 - T_2)\sqrt{\rho C}} \right)^2 \tag{23}
$$

For the experimental results, in order to limit the fluctuations of k_{hot} due to the limited resolution of the thermocouple, the value of k_{hot} at t has been evaluated from the temperatures T_1 and T_2 at times $t_1 = t - 36$ s and $t_2 = t + 36$ s. For the theoretical results, resolution is not an issue, so we used $t_1 = t - 2$ s and $t_2 = t + 2$ s. An analysis of the influence of the different parameters has also been conducted.

A. Description of the Low-Density Thermal Insulators Studied

Measurements have been made on four different EPS foams in which radiative heat transfer has been proven to play a significant part in the total heat transfer [7]. The EPS foams used have been previously characterized. Their equivalent thermal conductivities $k_{\text{eq},m}$ have been measured by the guarded hot-plate method for an average temperature of 296 K. These equivalent conductivities can be taken as references. The global radiative properties of the foams β, ω, and $P(\nu)$ needed for the numerical simulation have been determined theoretically in a previous study [7], from their measured structural characteristics such as density or mean cell diameter. The validity of the model used has been checked by comparing experimental transmittance and reflectance measurements on thin slabs of foams with the calculated values obtained using the theoretical monochromatic radiative properties. Moreover, their conductive properties k_c have also been determined from a validated model of the literature [10], taking into account the conductivity of the constituents and the morphology of the foam. Thus, we could compute the theoretical equivalent thermal conductivity $k_{\text{eq,th}}$ from the radiative and conductive properties by solving numerically the steady-state one-dimensional coupled heat transfer equation using the discrete ordinates method in Cartesian coordinates and the control volume method. Given that the radiative contribution is relatively important in the EPS foams studied, their theoretical equivalent conductivity varies with the boundary conditions and, especially, with the average temperature of the material. For the

Table 1 Thermal characteristics of the four low-density EPS foams used

Sample no.	ρ, kg/m^3	$k_{eq,m}$, W/m/K at 296 K	β, m^{-1}	ω	g	b_1, W/m/K^3; b_2, W/m/K^2; b_3, W/m/K	$k_{eq,th}$, W/m/K at 296 K
1	10	0.0482	608.2	0.905	0.58	$b_1 = 8.878 \times 10^{-7}$; $b_2 = -2.09 \times 10^{-4}$; $b_3 = 0.0344$	0.05003
2	12.6	0.0428	763.9	0.901	0.58	$b_1 = 7.606 \times 10^{-7}$; $b_2 = -1.808 \times 10^{-4}$; $b_3 = 0.0328$;	0.04554
3	18.3	0.0396	1072.4	0.889	0.6	$b_1 = 5.308 \times 10^{-7}$; $b_2 = -9.081 \times 10^{-5}$; $b_3 = 0.02189$	0.04136
4	32.0	0.03395	$\beta_{ROSS} = 1400$	-	-	$b_1 = 2.636 \times 10^{-7}$; $b_2 = -2.46 \times 10^{-5}$; $b_3 = 0.01803$	0.03395

temperature range 296–320 K, the variations of $k_{eq,th}$, assuming black boundaries, for the four EPS foams have been proven to follow the form:

$$k_{eq,th} = b_1 T^2 + b_2 T + b_3 \tag{24}$$

where b_1 (W/m/K^3), b_2 (W/m/K^2), and b_3 (W/m/K) are constants peculiar to each foam.

All of the characteristics of the four EPS foams are shown in Table 1. Regarding sample no. 4, we checked that it is sufficiently dense to be considered as an optically thick medium, contrary to the other lighter samples. For this sample, the radiative heat transfer problem is then treated using the Rosseland approximation [14]. This approximation allows a direct relation between the radiative flux and the temperature gradient and greatly simplifies the calculation:

$$q_r^z = -\frac{16\sigma_{SB}}{3\beta_{ROSS}} T^3 \frac{\partial T}{\partial z}; \qquad q_r^x = -\frac{16\sigma_{SB}}{3\beta_{ROSS}} T^3 \frac{\partial T}{\partial x}; \qquad q_r^y = -\frac{16\sigma_{SB}}{3\beta_{ROSS}} T^3 \frac{\partial T}{\partial y} \tag{25}$$

B. Description of the Hot-Plane Apparatus

The hot-plane measuring system used is composed of different apparatuses (see Fig. 4): 1) the measuring apparatus, including the heated plane and a thermocouple placed at the center of the plane; 2) an intensity generator, supplying the hot plane with electric current; and 3) a data acquisition system connected to the thermocouples, allowing the recording of the temperature rise.

We used two different apparatuses that differ, among other things, by their area $L \times L$ (plane 1, $L = 0.25$ m and plane 2, $L = 0.125$ m). Plane 2 was usually used for measurements on opaque materials, whereas plane 1 was specially made for this study. The heated planes are composed of a curved track of constantan of known width and thickness in a serpentine pattern in a slab of kapton (see Fig. 4). Note that the heat is not generated homogeneously, as the Joule effect only occurs in the constantan element. However, owing to the homogeneous distribution of the constantan on the area of the plane, it is assumed that the heat is homogeneously dissipated in the plane. To take into account, as faithfully as possible, the inertia of the planes, the thermophysical properties of the planes $\rho_p C_p$ and k_p are assumed to be homogeneous and are calculated by averaging the properties of the two components (kapton and constantan).

For plane 1 with $L = 0.25$ m, which is composed of 82% constantan and 18% kapton, we have

$$\begin{aligned} \rho_p C_p &= 0.82 \times (\rho C)_{cst} + 0.18 \times (\rho C)_{kpt} = 0.82 \times (4.21 \times 10^6) \\ &\quad + 0.18 \times (1.548 \times 10^6) = 3.73 \times 10^6 \text{ J/(m}^3\text{K)} \\ k_p &= 0.82 \times k_{cst} + 0.18 \times k_{kpt} = 0.82 \times 19.5 + 0.18 \times 0.2 \\ &\approx 16 \text{ W/m/K} \\ h &= 100\ \mu\text{m} \end{aligned} \tag{26}$$

For the other plane (plane 2, $L = 0.125$ m), the percentage of constantan is 40% and the average thermophysical properties have been determined using the same assumptions:

$$\rho C_p = 2.596 \times 10^6 \text{ J/(m}^3\text{K)}; \qquad k_p \approx 7.8 \text{ W/m/K}; \qquad h = 280\ \mu\text{m} \tag{27}$$

The emissivity of the planes is difficult to determine precisely. However, in order to estimate it, we made reflectance measurements on the two faces of each plane for the radiation range $2\ \mu\text{m} < \lambda < 25\ \mu\text{m}$, which carries 93% of the radiative energy emitted at 300 K. This permitted us to determine a global emissivity in the infrared range calculated by averaging over all wavelengths. We found that $\varepsilon_p = 0.5$ for plane 1 and $\varepsilon_p = 0.1$ for plane 2. The value of the emissivity determined in this manner could appear relatively inaccurate, but we will see in Sec. V.D that the influence of the emissivity of the plane on transient heat transfer is relatively weak.

The intensity generator allowed us to supply the track of constantan with an electric current and to dissipate the heat rate by the Joule effect. The heat generated is proportional to the Ω_p (Ω) of the constantan track. These resistances have been measured using a

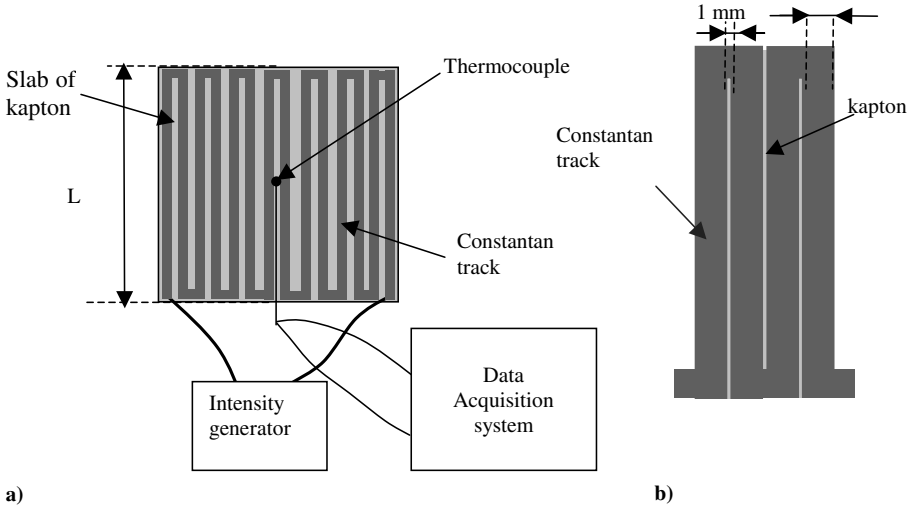

Fig. 4 Illustration of the structure of the a) hot-plane apparatus and b) heated plane 1.

multimeter and are, respectively, 42 and 101.3 Ω for plane 1 and plane 2. The heating power dissipated in the plane per unit area is then

$$\dot{Q} = W/2L^2 \tag{28}$$

V. Comparison of Experimental and Theoretical Results

We have measured the temperature rise of the two different hot-plane apparatuses with their two areas (plane 1 and 2) for each of the EPS foam samples presented. Measurements were made for the time range 1–600 s using a range of heating power $\dot{Q}$. The measurements were made by placing the hot-plane apparatus between two slabs of the foam sample considered. To ensure good thermal contact between the hot plane and the sample, the two slabs were slightly compressed using a heavy object. The dimensions of the foam slabs used are sufficiently large to consider that the porous medium surrounding the heated plane is infinite.

We also carried out corresponding theoretical calculations for each EPS foam sample, using the conductive and radiative properties and the foam densities illustrated in Table 1 and the properties of the planes presented in Sec. V.B. The other parameters necessary for the numerical solution are $T_{\text{init}} = 296$ K and

$$C = \frac{(\rho - \rho_{\text{air}})C_{\text{PS}} + \rho_{\text{air}}C_{\text{air}}}{\rho} \tag{29}$$

where $C_{\text{air}} = 1006$ J/kg/K and $C_{\text{PS}} = 1200$ J/kg/K.

The numerical parameters used are $nZ = 18$, $nY = nX = 20$, S_6 quadrature, $x_{\max} = y_{\max} = 0.3125$ m, and $z_{\max} = 0.15$ m for plane 1; whereas we used $nZ = 18$, $nY = nX = 18$, S_6 quadrature, $x_{\max} = y_{\max} = 0.28125$ m, and $z_{\max} = 0.15$ m for the simulations concerning plane 2. The values of $x_{\max}$, $y_{\max}$, and $z_{\max}$ have been chosen in order for the theoretical results to remain independent of their values. The results obtained then correspond to those of an infinite medium surrounding a finite plane area ($L \times L$). Finally, the theoretical calculations for a fictitious infinite plane ($L \to \infty$) have actually been carried out by setting $L = y_{\max} = x_{\max} = 10$ m.

A preliminary study in which the theoretical R_c at the plane/medium interface was varied has shown that R_c has almost no influence on the measurement as long as it is lower than 0.01 $\text{m}^2\text{K/W}$, whereas a bad thermal contact ($R_c > 0.01$ $\text{m}^2\text{K/W}$) could cause significant errors in the thermal conductivity measurement. However, in practice, the resistance at the interface may be significantly smaller than 0.01 $\text{m}^2\text{K/W}$, so that the heat transfer problem is not influenced by imperfect thermal contact. This assumption is checked by making several temperature measurements with different mechanical stresses applied to the EPS foam slabs sandwiching the plane in order to vary the thermal contact resistance. Experimental results show that the application of different mechanical loads has almost no influence on the temperature rise and, thus, that the real thermal contact resistance is too small to disturb the transient heat transfer. Thus, in all calculations, the thermal contact resistance between the plane and the surrounding medium will be neglected.

The comparisons of theoretical and experimental results concerning the evolution of the thermal conductivity k_{hot} estimated using the two different planes are illustrated in Figs. 5–8 for the four samples available. We also have depicted on these figures the theoretical (th) and experimental (exp) temperature rises of the planes. Moreover, for each foam sample, we have carried out the calculations assuming a fictitious infinite plane ($L \to \infty$) with the same thermophysical properties as plane 1. Finally, we also show on each figure the evolution of the theoretical equivalent conductivity $k_{\text{eq,th}}(T)$ [Eq. (24)], which would be measured by the guarded hot-plate method. The results depicted were obtained using a heating power $\dot{Q} = 31.4$ W/m^2 for measurements with plane 2 and $\dot{Q} = 29.6$ W/m^2 for plane 1.

The figures show that, whatever the foam sample, there is very good agreement between experimental and theoretical results for the temperature rise and the evolution of the estimated conductivity k_{hot}. Nevertheless, we note that for sample nos. 1, 2, and 3, the theoretical prediction tends to slightly overestimate the measured conductivity k_{hot}. This is not surprising and may be due to the fact that the radiative properties used slightly overestimate the radiative heat transfer, as shown in Table 1, in which we can see that the predicted conductivities $k_{\text{eq,th}}$ are a little larger than the measured ones.

Both theoretical and experimental results show that the evolution of the estimated conductivity k_{hot} is strongly dependent on the hot-plane apparatus used. Indeed, when using plane 2, for all foam samples, we observe first a decrease of the estimated conductivity k_{hot} for small measurement times (until t reaches approximately 200 s) followed by an increase of this conductivity that is always greater than the theoretical equivalent conductivity $k_{\text{eq,th}}$ stemming from the guarded hot-plate measurement. The increase of k_{hot} with t observed for plane 2 is too fast to be only attributed to the small increase of the effective thermal conductivity $k_{\text{eq,th}}$ with temperature [see Eq. (24)]. On the other hand, when plane 1 ($L = 0.25$ m) is used, the value of k_{hot} decreases and converges to a fixed value for sample nos. 3 and 4, whereas we only observe a very slight increase for sample nos. 1 and 2 at large t ($t > 500$ s). For all samples, we also note that the thermal conductivity estimated using plane 1 always exceeds the equivalent conductivity $k_{\text{eq,th}}$ stemming from the

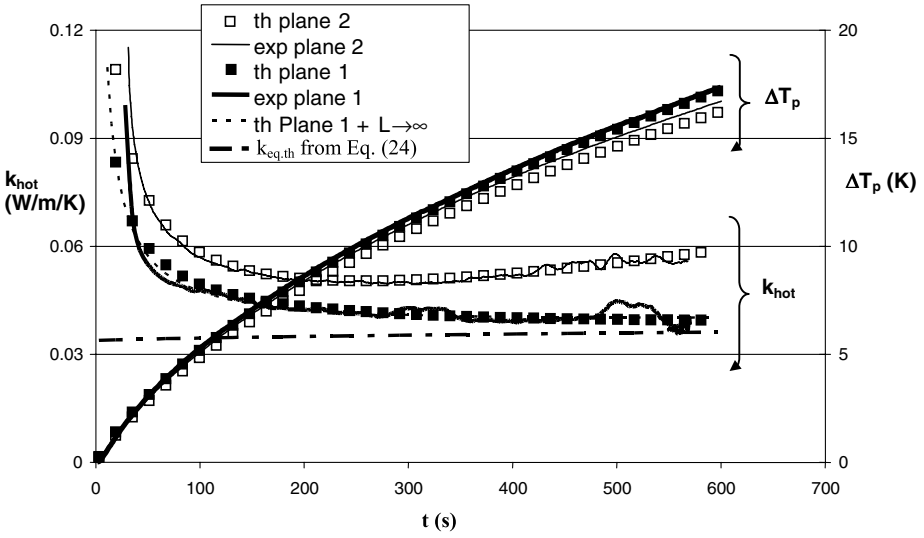

Fig. 5 Comparison of the temperature rise and estimated conductivity k_{hot} of sample no. 4 obtained experimentally and theoretically using two different hot planes.

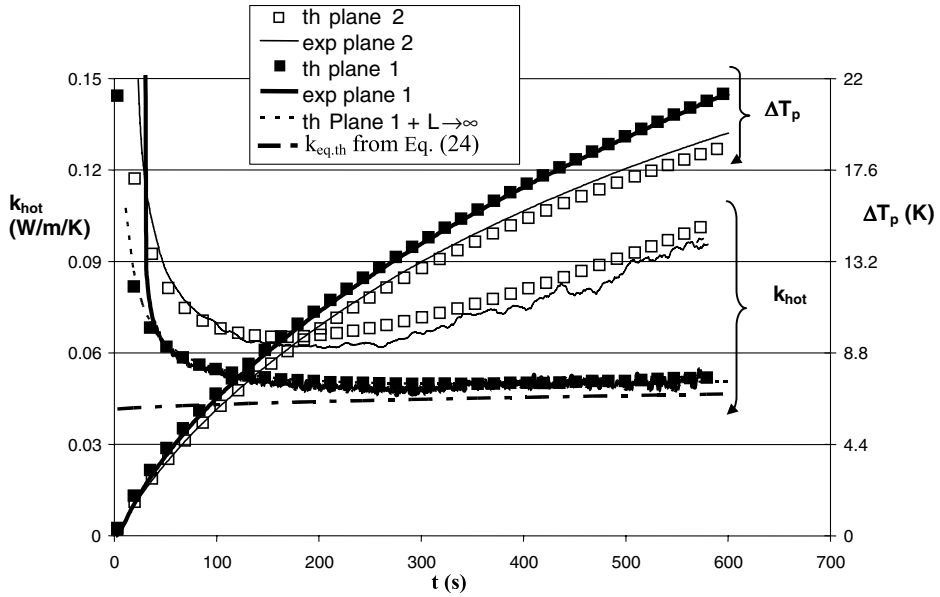

Fig. 6 Comparison of the temperature rise and estimated conductivity k_{hot} of sample no. 3 obtained experimentally and theoretically using two different hot planes.

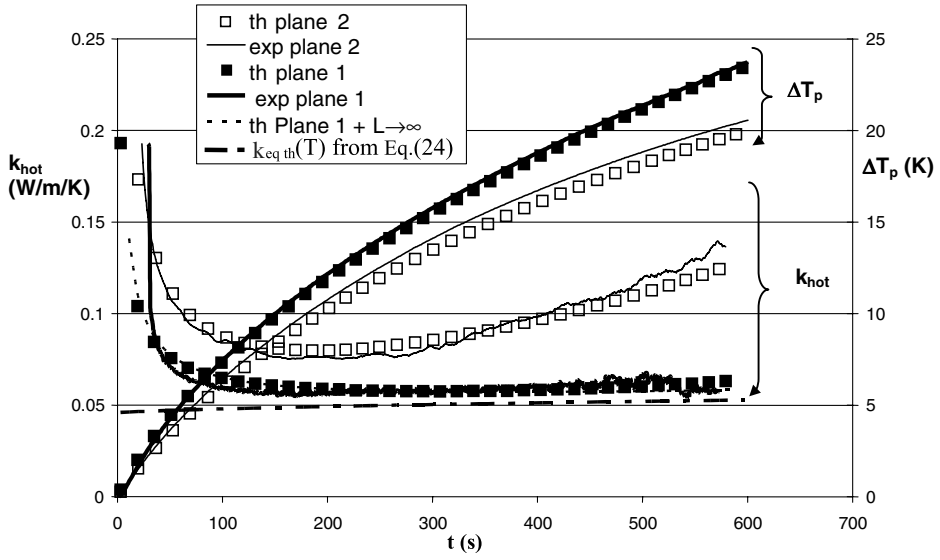

Fig. 7 Comparison of the temperature rise and estimated conductivity k_{hot} of sample no. 2 obtained experimentally and theoretically using two different hot planes.

guarded hot-plate measurement, but is always lower than the conductivity estimated using plane 2. At this stage, it is not possible to determine whether the difference observed between the results of the two planes and the thermal conductivity measured from the guarded hot-plate method are due to radiative phenomena or to limitations regarding the measuring apparatus.

To better understand the results observed, a more complete analysis of the influence of the different parameters, especially those related to the properties of foam used or to the measuring system, has to be conducted. Our numerical simulation will then be a very useful tool to analyze their theoretical influence and to explain the deviations observed for plane 2.

A. Influence of the Plane Area/Edge Effects

The hot-plane apparatus must be compact in order to make measurements on relatively small samples. That is the reason why the usual area $L \times L$ of the heated plane is limited. In classical hot-plane measurement on purely conductive materials, planes with a maximum area of $L \times L \approx 160$ cm^2 ($L = 0.125$ m) are generally used. It is usually assumed that the plane is large enough to consider that the heat transfer remains one-dimensional during the measurement duration and that edge effects can be neglected. The analysis of the results of Figs. 5–8 shows that this assumption is no longer valid when measurements are made on low-density thermal insulators. Indeed, as can be observed in the four figures, noticeable difference are found between the evolutions of k_{hot} estimated using the different apparatuses. For small t, the difference observed between the results of plane 2 ($L = 0.125$ m) and plane 1 ($L = 0.25$ m) are mainly due to inertia effects that are more important for the former apparatus. On the other hand, for large t, inertia effects become negligible, and the differences observed indicate that the assumption of one-dimensional heat transfer is wrong when using the hot-plane apparatus with $L = 0.125$ m on these types of porous materials.

Edge effects are characterized by an abnormal increase in the estimated conductivity k_{hot} with time. This increase is much faster than the increase of the effective thermal conductivity of the foam $k_{eq,th}$ with temperature due to radiative phenomena [see Eq. (24)].

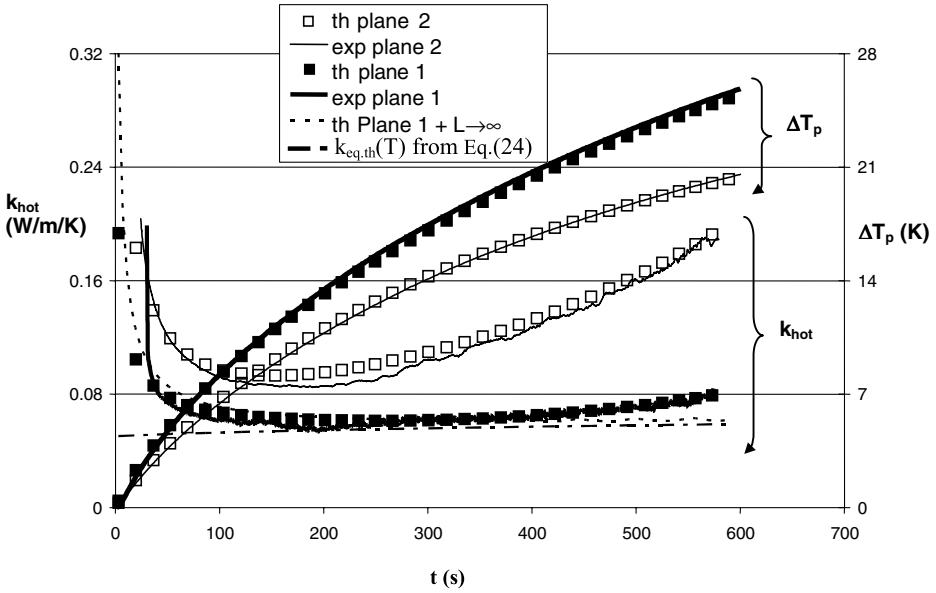

Fig. 8 Comparison of the temperature rise and estimated conductivity k_{hot} of sample no. 1 obtained experimentally and theoretically using two different hot planes.

The influence of edge effects is significant even for relatively small t. For example, the theoretical results indicate that, for sample no. 3, the relative difference between k_{hot} estimated using plane 2, or using a fictitious infinite plane with the same other thermophysical properties, exceeds 10% as soon as t is greater than 130 s and reaches 108% at $t = 600$ s. These observations clearly show that the classical hot-plane measurement method ($L \leq 0.125$ m) applied to such low-density insulating materials does not permit determination of a satisfactory equivalent thermal conductivity, as the thermal conductivity k_{hot} estimated by the classical hot-plane method does not converge to a constant value, but shows a continuous increase with the measurement t. Then, two measurements made at different times will lead to different values of the thermal conductivity.

Moreover, experimentally and theoretically, it appears that a plane with $L = 0.25$ m is sufficient to avoid edge effects during all measurement time ($t \leq 600$ s) for sample nos. 3 and 4. Indeed, as can be observed in Figs. 5 and 7, the theoretical evolutions of k_{hot} are almost identical when $L = 0.25$ m and $L \to \infty$ (thermal inertia of plane 1) for sample no. 4, whereas for sample no. 3, a very slight difference is observed when t reaches large values ($t > 500$ s). The relative differences in both cases are, respectively, 0.4% and 2.6% at $t = 600$ s. On the other hand, for sample nos. 1 and 2, edge effects are still significant even when measurements are made using plane 1. For instance, the relative differences between k_{hot} for $L = 0.25$ m and k_{hot} for $L \to \infty$ at $t = 600$ s are 8.8% and 24%, respectively.

Theoretical and experimental results show that the influence of edge effects is more pronounced when measurements are made on materials with very low density, as the increase of k_{hot} with measurement t is faster than for heavier foam. This remark is valid regardless of the area of the plane. To investigate more rigorously the influence of the density of the material, we carried out numerical simulations of the temperature rise for fictitious materials for which density varied from 10 to 100 kg/m^3, using hot-plane apparatuses with length $L = 0.125$, 0.25, and 0.35 m and $L \to \infty$. The other properties of these materials were those of sample no. 3, presented in Sec. V.A, and remained constant so that we only investigated the influence of the density. The heating power was $\dot{Q} = 29.6$ W/m^2. The results are illustrated in Table 2, in which we show the evolution (as a function of ρ) of the relative differences between the estimated conductivity k_{hot} at $t = 600$ s obtained for a finite plane ($L = 0.125$, 0.25, or 0.35 m) and assuming an infinite plane, for the fictitious materials previously described.

These theoretical results confirm that when using a standard hot-plane apparatus ($L = 0.125$ m), edge effects may be significant even for materials with densities over 50 kg/m^3. The classical hot-plane method is then poorly adapted to materials with low density. On the contrary, when the length of the plane is 0.25 m, edge effects are almost negligible as long as the density of the material is greater than approximately 15 kg/m^3. For porous materials with lower densities, planes with larger dimensions are required to avoid edge effects.

B. Influence of the Inertia of the Plane

As was explained in Sec. III.A, the thermal inertia of the plane per unit area ($\rho_p C_p h$ in J/m/K) must be negligible in order for the usual hot-plane method to be rigorously applicable. In practice, the planes used have a certain inertia, as was observed in the previous paragraph when we compared the evolution of k_{hot} using the two different apparatuses (1 and 2) at small time. However, inertia effects are especially significant at the beginning of the heating (small time) when the temperature of the plane increases rapidly. When time is sufficiently large, the temperature rise gets slower, and the proportion of energy used to heat the plane becomes negligible so that Eq. (4) could be used without causing errors. The heating duration necessary for inertia effects to be negligible is related to the inertia of the plane and to the inertia of the porous medium (ρC) as well. To estimate this time, we carried out calculations of the temperature rise in sample no. 4 using fictitious planes with length $L = 0.25$ m and with different values of thermal inertia per unit area of the plane ($\rho_p C_p h$). The results are illustrated in Fig. 9 for a heating power $\dot{Q} = 29.6$ W/m^2.

The theoretical results of Fig. 9 for sample no. 4 indicate that, for measurements on low-density EPS foam, planes with relatively small inertia have to be used. When measurements are made using a plane with a thermal inertia $\rho_p C_p h$ close to that of plane 1 or plane 2, a measurement time of $t = 600$ s is not sufficient for the inertia effects to be negligible. Indeed, the theoretical errors caused by inertia effects are approximately 5.5% and 10.2% when using plane 1

Table 2 Theoretical evolution of the relative error due to edge effects at $t = 600$ s for different plane lengths and for fictitious materials with different densities

	ρ, kg/m^3				
Length L, m	10	18.3	25	50	100
0.125	148%	108%	66%	35.2%	17%
0.25	11.6%	2.6%	1.3%	0.6%	0.05%
0.35	1.5%	0.25%	0.1%	0%	0%
∞	0%	0%	0%	0%	0%

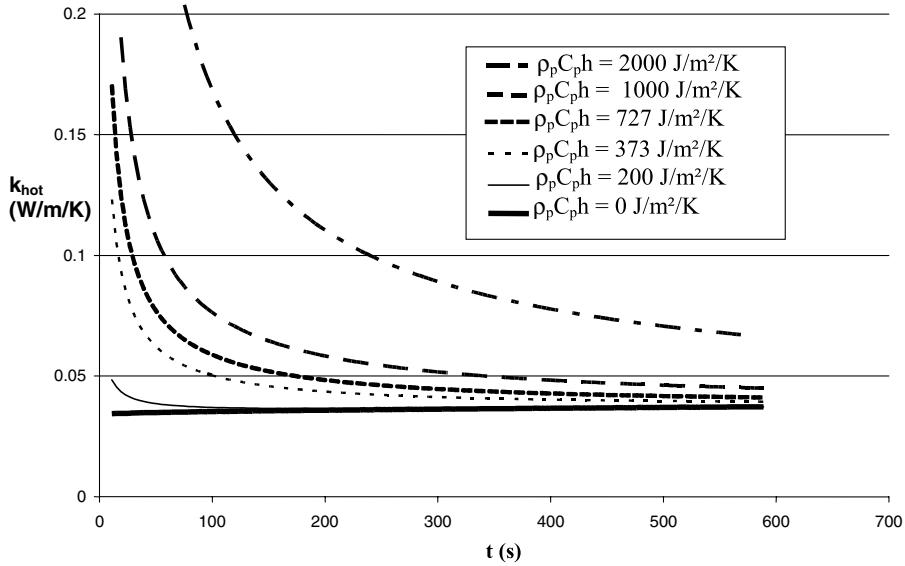

Fig. 9 Theoretical evolution of the estimated conductivity k_{hot} of sample no. 4 using planes with length $L = 0.25$ m and with different values of thermal inertia per unit area $\rho_p C_p h$.

and plane 2, respectively. This error reaches 20.9% and 78% when the thermal inertia $\rho_p C_p h$ of the plane is 1000 J/m^2/K or 2000 J/m^2/K, respectively. Standard planes are then not fit for the measurement of the thermal conductivity of low-density thermal insulators. On the other hand, if we used a hot plane with a heat capacity per unit area equal to 200 J/m^2/K, the error at $t = 600$ s would be only 0.5%.

We also investigated the influence of the heat capacity of the porous medium on the evolution of the error caused by inertia effects, by carrying out numerical simulations for the three other foam samples using the previous fictitious planes. The results are illustrated in the Table 3, in which we show the relative error due to inertia effects found at $t = 600$ s when using plane 1 ($\rho_p C_p h = 373$ J/m^2/K and $L = 0.25$ m) or a plane with length $L = 0.25$ m having the same thermal inertia as plane 2 ($\rho_p C_p h = 727$ J/m^2/K).

As can be seen, the relative error due to inertia effects varies slightly with the inertia of the porous medium. Indeed, whatever the heat capacity of the plane, the theoretical error due to inertia effects on the estimation of k_{hot} at $t = 600$ s decreases when the density of the porous medium increases. To conclude, a plane with a small inertia is required.

C. Influence of the Heating Power

We experimentally and theoretically investigated the influence of the heating power on the hot-plane measurement by measuring and calculating the temperature rise for other values of $\dot{Q}$: $\dot{Q} = 60$ W/m^2 and $\dot{Q} = 15$ W/m^2. The theoretical and experimental results regarding the evolution of the estimated thermal conductivity k_{hot} of sample no. 4 using plane 2 are illustrated in Fig. 10 for the three values of power used.

As can be seen, the power used for heating the plane has a slight influence on the estimated thermal conductivity. Nevertheless, it appears both experimentally and theoretically that a high heating power tends to increase k_{hot}. For example, when the power supplied is $\dot{Q} = 60$ W/m^2, the predicted conductivity k_{hot} at $t = 400$ s is approximately 2 mW/m/K higher than when $\dot{Q} = 30$ W/m^2. This difference is nearly the same for a finite plane ($L = 0.125$ m) or an infinite plane. For experimental results, the difference is difficult to estimate, as the measured values fluctuate, but the difference is the same order of magnitude as the predictions and the agreement with the numerical simulation proves to be satisfactory again.

The influence of $\dot{Q}$ could be explained by the fact that when the heating power gets larger, the temperature reached near the plane is higher, and the radiative energy emitted by the plane and the porous medium (which varies by T^4) is larger. Thus, the total heat transferred from the plane to the surrounding medium is larger, and the surrounding material behaves as if its conductivity k_c were higher. In conclusion, one has to be very attentive to the heating power used for the measurement in order for the temperature reached to be close to that desired for the measurement of the thermal conductivity.

D. Influence of Radiative Heat Transfer on Hot-Plane Measurement

The comparison between experimental and theoretical results, which we conducted in the previous sections, has shown that the model developed provides satisfactory simulations of the temperature rise of the plane. Thus, we could use it to investigate the influence of the radiative contribution on the classical measurement of the estimated thermal conductivity k_{hot} that is, theoretically, only applicable to a purely conductive medium. To do that, we carried out the theoretical calculations for four fictitious purely conductive materials (nos. 5, 6, 7, and 8) having the same theoretical equivalent conductivity $k_{eq,th}(T)$ [see Eq. (24)] and the same thermophysical properties ρ and C as the foams previously studied. The calculations were made using sufficiently large and thin planes to avoid inertia and edge effects. Then, we used fictitious ideal planes with $L =$

Table 3 Theoretical relative error, due to inertia effects, made on the conductivity k_{hot} estimated at $t = 600$ s using plane 1 or plane 2 with $L = 0.25$ m for each foam sample

	Sample no.			
Inertia of the plane, J/m^2/K	1 ($\rho = 10$ kg/m^3)	2 ($\rho = 12.6$ kg/m^3)	3 ($\rho = 18.3$ kg/m^3)	4 ($\rho = 32$ kg/m^3)
$\rho_p C_p h = 727$	16%	15%	12.5%	10.2%
$\rho_p C_p h = 373$	7.9%	7.4%	6.4%	5.5%
$\rho_p C_p h = 0$	0%	0%	0%	0%

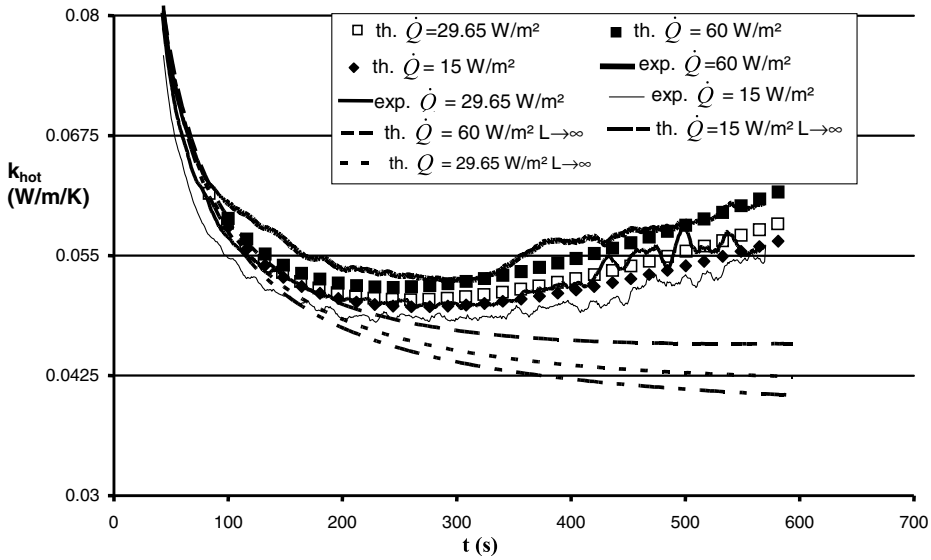

Fig. 10 Evolution of the theoretical and experimental thermal conductivity k_{hot} measured with plane 1 for sample no. 4 and different heating power values.

0.25 m for sample no. 4, $L = 0.3$ m for sample no. 3, and $L = 0.35$ m for sample nos. 1 and 2.

The other characteristics of the optimized planes were

$$h = 100\ \mu\text{m}; \qquad \rho_p C_p = 2.36 \times 10^6\ \text{J/(m}^3\text{K)}; \qquad k_p \approx 10\ \text{W/m/K}; \qquad \varepsilon_p = 1.0 \tag{30}$$

The evolutions of the temperature and of the estimated conductivity k_{hot} obtained for sample nos. 5, 6, 7, and 8 have been compared with those calculated for the four corresponding EPS samples, in which radiative heat transfer is significant. The thermal conductivity k_c of the fictitious materials nos. 5, 6, 7, and 8 were equal to the equivalent conductivity of sample nos. 1, 2, 3, and 4:

$$k_c(T) = b_1 T^2 + b_2 T + b_3 \tag{31}$$

where b_1, b_2, and b_3 are given in Table 1 for foam sample nos. 1, 2, 3, and 4.

In the numerical model, as the radiative contribution is assumed null, we set $\boldsymbol{q}^t_{r_{i,j}} = \mathbf{0}$ and $(\nabla \boldsymbol{q}_r)^t_{i,j} = 0\ \forall\ t$, i and j. The numerical parameters used for the calculations were $nZ = 18$; $nX = nY = 20$; S_6 quadrature; $z_{max} = 0.15$ m for all samples and $y_{max} = x_{max} = 0.5$ m for sample nos. 1, 2, 5, and 6 ($L = 0.4$ m); $y_{max} = x_{max} = 0.4$ m for sample nos. 3 and 7 ($L = 0.3$ m), and $y_{max} = x_{max} = 0.3125$ m for sample nos. 4 and 8 ($L = 0.25$ m).

The other parameters were $\dot{Q} = 29.6\ \text{W/m}^2$, $R_c = 0\ \text{K/W}$, and $T_{init} = 296$ K, and the numerical parameters were those used in Sec. VI.

The evolution of k_{hot} for the fictitious purely conductive materials and the corresponding EPS foams are illustrated in Fig. 11a. For each foam, we also show the variation of the equivalent conductivity that would be obtained from guarded hot-plate measurements.

The comparison of the results in Figs. 11a and 11b shows that, during the hot-plane measurement, there are notable differences between the behavior of purely conductive materials and materials for which radiative heat transfer is significant even when the two materials have the same equivalent thermal conductivity and the same thermophysical properties.

Regarding the evolution of the temperature in Fig. 11b, one can notice that, for a given heating power, the temperature of the plane reaches lower values when the surrounding medium is purely conductive than reached when there is radiation/conduction coupling. The difference is more important for the lighter foams in which the radiative contribution is more important, but remains relatively small. For sample nos. 1 and 5, this difference reaches 0.3 K at $t = 600$ s, whereas it is almost negligible (<0.1 K) for sample nos. 4 and 8. The very slight difference observed between the temperature rise for sample nos. 4 and 8 could be explained by the fact that sample no. 4 is sufficiently opaque to be considered as optically thick. Then, the Rosseland approximation is valid and, although radiative transfer is not negligible in this sample, the total heat transfer follows Fourier's law. Actually, the material behaves in a purely conductive manner with a conductivity $k = k_c + k_{ROSS}$ [Eq. (24)]. On the other hand, when the optical thickness of the materials remains small, the radiative transfer follows more complex laws, and the thermal behavior of the material differs from that of a purely conductive medium.

Concerning the evolution of the estimated conductivity k_{hot} in Fig. 11a, some important differences are also found when radiative heat transfer occurs, especially for short time. As for the temperature rises, these differences are more pronounced for the lighter foams and are almost negligible for sample nos. 4 and 8. Moreover, for short time ($t < 200$ s), when the influence of the inertia of the plane remains important, the theoretical k_{hot} obtained for the purely conductive materials is greater than for the corresponding EPS foam. This difference is explained by the fundamentally different nature of the conductive heat transfer and radiative heat transfer in nearly transparent materials. However, one can observe that, as the measurement time reaches large values, the estimated conductivities k_{hot} of the foam samples tend to that computed for the corresponding purely conductive materials. At $t = 600$ s, the relative differences between the conductivities k_{hot} estimated for the purely conductive materials and semitransparent foams are, respectively, 0.2, 0.1, 0.1, and 1.0% for sample nos. 1, 2, 3, and 4. These differences are negligible and might be due to the fact that the temperatures of the plane are not exactly the same for the purely conductive materials as for the foams. One can also see that when the inertia of the plane becomes negligible, the estimated conductivity k_{hot} for the foam samples follows the evolution of the equivalent conductivity $k_{eq,th}$ with the temperature expressed by Eq. (24).

As a consequence, it can be concluded that, if an estimate of k_{hot} is made after a sufficiently large time, the thermal conductivity estimated by the hot-plane method is in close agreement with the equivalent thermal conductivity $k_{eq,th}$ measured from a guarded hot-plate method. Thus, it appears from the theoretical results that the hot-plane method could be extended to media in which the radiation/conduction coupling occurs even when the Rosseland approximation is not valid. Moreover, in comparison with the guarded hot-plate method, the hot-plane method could theoretically give additional information on the semitransparent medium, as it permits measuring the evolution of the equivalent conductivity as a function of the temperature by making measurements at different times or with

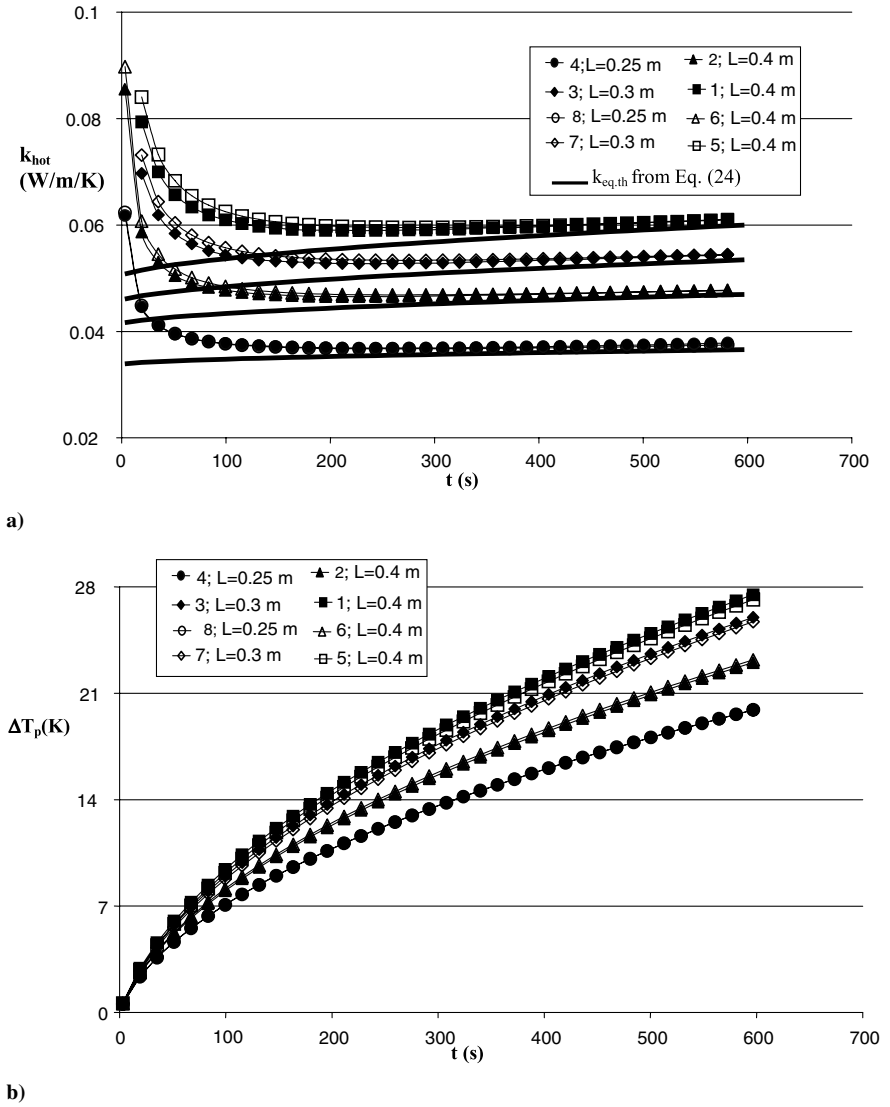

Fig. 11 Theoretical evolutions of purely conductive materials nos. 5, 6, 7, and 8 and the corresponding EPS foams sample nos. 1, 2, 3, and 4 using an optimized plane for a) estimated conductivity k_{hot} and b) temperature.

different values of heating power. Thus, it could be a very interesting method for characterizing in a more detailed manner the heat transfer in the medium, because the increase of equivalent thermal conductivity with temperature is closely related to the importance of radiative transfer. Furthermore, the low-limit value of the time at which the measurement should be made depends on the foam considered. As was explained in Sec. V.B, for light foams, the effect of the inertia of the plane is more significant.

The previous numerical calculations have been carried out assuming that the plane constituting the measurement apparatus was perfectly black ($\varepsilon_p = 1$). This parameter directly influences the radiant energy emitted by the plane and could affect the radiative transfer problem. Thus, in order to analyze the influence of the emissivity of the plane on the hot-plane measurement, we made theoretical calculations for each foam assuming different emissivities ranging from 1 to 0.

The results show that the emissivity of the plane has actually a weak influence on the evolution of the estimated conductivity k_{hot}. This influence is significant especially at low measurement time ($t < 300$ s) and when the emissivity of the plane reaches very low values ($\varepsilon_p < 0.5$). It is characterized by lower values of k_{hot} when the plane is less emissive. For example, at $t = 100$ s, the theoretical differences between k_{hot} measured using perfectly emissive and nonemissive planes are 4.8, 3.1, 1.8, and 0.06 mW/m/K for sample nos. 1, 2, 3, and 4, respectively. This could be explained by the fact that the radiant energy emitted by the plane (and, thus, the heat transferred by radiation) is smaller when the emissivity of the plane decreases. As expected, it was found that the theoretical influence is more pronounced for light foams in which radiative transfer is more important. However, we remark that when the measurement time reaches large values ($t \to 600$ s), the conductivity k_{hot}, measured using a nonemissive plane, converges on that obtained with a perfectly black one. Indeed, at $t = 600$ s, the differences are only 1.2 mW/m/K (2%), 0.9 mW/m/K (1.7%), 0.44 mW/m/K (1%), and 0.57 mW/m/K (1.5%) for foam sample nos. 1, 2, 3, and 4, respectively.

These differences are relatively small. Moreover, nonemissive planes are very difficult to obtain. As a consequence, in practice, we could assume without significant error that the emissivity of the plane has almost no influence on the estimated conductivity.

VI. Conclusions

The hot-plane method is a technique for measuring the equivalent thermal conductivity. It is theoretically restricted to purely conductive materials (opaque media). This represents one of the most important drawbacks of the method, given that numerous thermal insulators used in the building industry, such as EPS foams or light fibrous materials, are among this type of porous media. At present, no study has previously been conducted to investigate the application of this measuring method to low-density porous media in which both conductive and radiative heat transfer occurs. In this

article, we both theoretically and experimentally studied the use of this technique on low-density EPS foams.

The theoretical and experimental results shown in the previous sections permitted us to evaluate the influence of parameters such as the density of the material, the area of the plane, the thermal inertia of the plane, the heating power, and the thermal contact resistance on the evolution of the estimated thermal conductivity k_{hot} of the material. For each of these parameters, the experimental results are well predicted by the numerical model simulating 3-D transient coupled heat transfer. Thus, the model proves to be a useful tool to theoretically investigate the application of the hot-plane method to light, porous materials in which both conductive and radiative transfer occurs.

The experimental and theoretical investigations revealed that classical hot-plane apparatuses are poorly adapted to k_{eq} measurements on thermal insulators for which densities are lower than 50 kg/m^3, given that the maximum area of classical hot planes ($L = 0.125\ \text{m} \rightarrow L \times L \approx 160\ \text{cm}^2$) is not sufficient to avoid edge effects. A minimum area of 1200 cm^2 ($L = 0.35$ m) may be required in order to make satisfactory measurements on very light foams ($\rho = 10\ \text{kg/m}^3$), whereas planes with areas close to 600 cm^2 are sufficient for heavier foams ($\rho = 30\ \text{kg/m}^3$). Theoretical and experimental results also showed that, for such materials, the errors caused by the thermal inertia of the plane could be significant when using standard planes such as plane 1 or plane 2 even when the estimate of k_{hot} is made at $t = 600$ s. Thinner planes with a sufficiently small thermal inertia per unit length have to be used to give accurate results. Thus, relatively large ($L \geq 0.3$ m) and thin ($\rho_p C_p h \leq 300\ \text{J/m}^2\text{/K}$) planes are required for measurements on low-density thermal insulators.

Finally, we also investigated the influence of radiative heat transfer on measurement by comparing the thermal behavior of the EPS foams with that of fictitious purely conductive materials with the same thermophysical properties and the same equivalent thermal conductivities. The theoretical results showed that, when the foam was too transparent to behave as an optically thick material (Rosseland approximation), the temperature of the plane was slightly different and reached higher values than for the corresponding fictitious purely conductive material. The conductivities k_{hot} for the fictitious purely conductive materials were somewhat greater than those obtained for the corresponding real foams for short measurement time. Nevertheless, in both cases (fictitious purely conductive foam and real foam), when measurement time reached large values, the theoretical conductivity k_{hot} converged on the equivalent thermal conductivity $k_{\text{eq,th}}$ stemming from the simulation of the guarded hot-plate method. Moreover, k_{hot} followed the evolution of $k_{\text{eq,th}}$ with the temperature. Then, if the estimate of k_{hot} were made at sufficiently large time, the result of the hot-plane method was in close agreement with the equivalent conductivity obtained from the guarded hot-plate measurement.

As a consequence, providing that the plane used is sufficiently long and has a sufficiently small heat capacity per unit area, this measuring method could be extended to media in which conductive and radiative transfers occur simultaneously. Moreover, contrary to the guarded hot-plate method, the hot-plane method could give additional information concerning the evolution of the equivalent conductivity of the material by estimating the value of k_{hot} at different times.

References

[1] Klarsfeld, S., "Guarded Hot Plate Method for Thermal Conductivity Measurements," *Compendium of Thermophysical Property Measurement Methods*, edited by K. D. Maglic, A. Cezairliyan, and V. E. Peletsky, Recommended Measurement Techniques and Practices, Vol. 2, Plenum, New York, 1992, pp. 99–131.

[2] Rudajevová, A., von Buch, F., and Mordike, B. L., "Thermal Diffusivity and Thermal Conductivity of MgSc Alloys," *Journal of Alloys and Compounds*, Vol. 292, Nos. 1–2, 1999, pp. 27–30.

[3] Yamanaka, S., Yamada, K., Kurosaki, K., Uno, M., Takeda, K., Anada, H., Matsuda, T., and Kobayashi, S., "Thermal Properties of Zirconium Hydride," *Journal of Nuclear Materials*, Vol. 294, Nos. 1–2, 2001, pp. 94–98.

[4] Lazard, M., André, S., and Maillet, D., "Diffusivity Measurement of Semi-Transparent Media: Model of the Coupled Transient Heat Transfer and Experiments on Glass, Silica Glass and Zinc Selenide," *International Journal of Heat and Mass Transfer*, Vol. 47, No. 3, 2004, pp. 477–487.

[5] He, Y., "Rapid Thermal Conductivity Measurement with a Hot Disk Sensor, Part 1: Theoretical Considerations," *Thermochimica Acta*, Vol. 436, Nos. 1–2, 2005, pp. 122–129.

[6] Kohout, M., Collier, A. P., and Štěpánek, F., "Effective Thermal Conductivity of Wet Particle Assemblies," *International Journal of Heat and Mass Transfer*, Vol. 47, No. 25, 2004, pp. 5565–5574.

[7] Xuan, Y., and Li, Q., "Heat Transfer Enhancement of Nanofluids," *International Journal of Heat and Fluid Flow*, Vol. 21, No. 1, 2000, pp. 58–64.

[8] Azhar-Ul-Haq, Saxena, N. S., Gustafsson, S. E., and Maqsood, A., "Simultaneous Measurement of Thermal Conductivity and Thermal Diffusivity of Rock-Marbles Using Transient Plane Source (TPS) Technique," *Heat Recovery Systems and CHP*, Vol. 11, No. 4, 1991, pp. 249–254.

[9] Saleh A. Al-Ajlan, "Measurements of Thermal Properties of Insulation Materials by Using Transient Plane Source Technique," *Applied Thermal Engineering*, Vol. 26, Nos. 17–18, 2006, pp. 2184–2191.

[10] Coquard, R., and Baillis, D., "Modelling of Heat Transfer in Low-Density EPS Foams," *Journal of Heat Transfer*, Vol. 128, No. 6, June 2006, pp. 3279–3290.

[11] Carslaw, H. S., and Jaeger, J. C., *Conduction of Heat in Solids*; 2nd ed., Oxford Univ. Press, Oxford, 1959.

[12] Viskanta, R., and Lim, J., "Transient Cooling of a Cylindrical Glass Gob," *Journal of Quantitative Spectroscopy and Radiative Transfer*, Vol. 73, No. 2-5, 2002, pp. 3279–3290.

[13] Ozisik, M. N., *Radiative Transfer and Interaction with Conduction and Convection*, Wiley, New York, 1973, p. 575.

[14] Hottel, H., and Sarofim, A. F., *Radiative Transfer*, McGraw–Hill, New York, 1967.

[15] Chin, J. H., Panczak, T. D., and Fried, L., "Finite Element and Ray-Tracing in Coupled Thermal Problem," *Proceedings of the Sixth International Conference on Numerical Methods in Thermal Problems*, Pineridge , Swansea, Wales, U.K., 1989, pp. 683–701.

[16] Chandrasekhar, S., *Radiative Transfer*, Dover, New York, 1960.

[17] Ayranci, I., and Selçuk, N., "MOL Solution of DOM for Transient Radiative Transfer in 3-D Scattering Media," *Journal of Quantitative Spectroscopy and Radiative Transfer*, Vol. 84, No. 4, 2004, pp. 409–422.

[18] Kim, S. H., and Huh, K. Y., "A New Angular Discretization Scheme of the Finite Volume Method for 3-D Radiative Heat Transfer in Absorbing, Emitting and Anisotropically Scattering Media," *International Journal of Heat and Mass Transfer*, Vol. 43, No. 7, 2000, pp. 1233–1242.